SIMULATION TOOLS FOR HIGH-INTENSITY RADIOGRAPHIC DIODES*

Stanley Humphries, Field Precision, Albuquerque, NM 87192 USA and
Thaddeus Orzechowski and James McCarrick, Lawrence Livermore National Laboratory,
Livermore, CA 94551 USA

Abstract

Version 6.0 of the Trak 2D ray-tracing code has new features to address simulations of intense electron beam diodes for radiography. The modifications support a program at LLNL to develop small radiographic sources for interior illumination. The application requires a pulsed electron beam (>15 kA, 30 ns, 1.2 MeV) confined to a three-dimensional focus less than 1 mm in dimension. Two key concepts make the application feasible: a magnetically-insulated transmission line for connection to the pulsed-power generator and a coaxial pinched-beam diode for axial localization of electrons. New capabilities in Trak include high-accuracy calculations of beam-generated magnetic fields with the effects of non-laminar or reflex electron orbits and current flow in the anode target. The program supports multiple space-charge emission surfaces to model effects of ion backflow. Models for electron backscatter from the tungsten target have also been implemented. Simulations indicate that the requirements can be achieved with reasonable anode/cathode gaps (> 4 mm).

CRAD -- COMPACT RADIOGRAPHIC DIODE

We describe computation work in support of a project at Lawrence Livermore National Laboratory to develop pulsed X-ray sources for radiography with internal illumination. Experimental work is currently in progress at LLNL under the direction of Timothy Houck. The application requires the transport of about 20 GW of pulsed power to an electron diode over lengths greater than 1 m with a maximum available transverse dimension less than 8 cm. The diode must generate more than 15 kA of electrons at 1.2 MV with transport to a spot less than 1 mm in width. Our approach has three key components:

- an applied-field magnetically-insulated transmission line for power transport,
- a narrow anode rod for small radial spot size, and
- a diode geometry that ensures electron self-pinching to achieve a small axial spot size.

Figure 1 shows the transmission line cross-section. With an applied field of 0.6 tesla the assembly has been shown to withstand pulsed electric fields exceeding 1 MV/cm.

The computations discussed in this paper address the third issue, optimum diode geometries to ensure electron pinches at relatively high impedance (50 Ω).
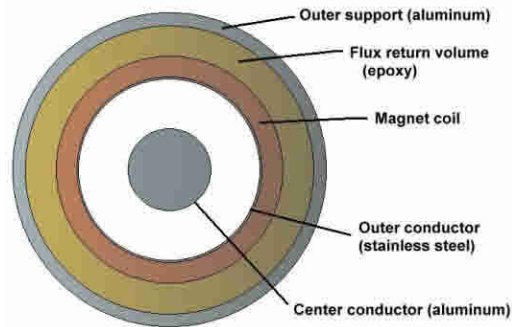

Figure 1. Magnetically-insulated transmission line, outer diameter 7.6 cm

FEATURES OF TRAK

The Trak 2D ray tracing code has been under development for over 10 years and is now in Version 6.0. Trak is an integrated package for mesh generation, electric and magnetic field solution and orbit tracking with self-consistent effects of beam fields. The programs constitute a fully interactive graphical working environment. The foundation of the codes is the application of finite-element methods on conformal meshes. The approach gives precise field calculations on material surfaces for accurate simulations of space-charge-limited and field emission. The following new features of Version 6.0 address CRAD simulation requirements:

- increased flexibility for multi-species particle generation,
- advanced methods to find the magnetic fields of relativistic beams on conformal meshes, and
- inclusion of electron backscatter from the tungsten target.

Regarding the first feature, users can now enter particle parameters manually from a list and/or request automatic generation from emission surfaces in any of the particle tracking modes. In the space-charge mode current is assigned to emission-surface particles following the Child-law prescription with the option for local source limits. An emission surface in Trak is a set of contiguous nodes on an electrode that have a unique region number. Emission facets are the boundaries between material and vacuum elements that connect the nodes. Trak automatically identifies and organizes facets and then divides them into segments associated with model particles. The code supports up to twenty emission surfaces that can each be assigned a particle species, a source limit and an angular divergence. With this

flexibility it is straightforward to model the space-charge-limited counter-flow of ions and electrons. Trak uses an adjustable time step for particle integration so there is no penalty for a large difference in mass.

The calculation of beam-generated magnetic fields is based on the assignment of model particle currents to element facets intersected by the orbits. Current enclosed within a node can be determined by taking an integral along facets to the axis. Current assignment on the conformal mesh preserves zero divergence of current density and unambiguously defines the sense of current with respect to the axial direction. These features are necessary to model the complex reflex orbits of electrons in a pinched beam. The program also assigns current to the source and target facets intersected by the orbits. The values are used to determine surface current flow on conducting boundaries and structures. In addition, the facet currents on the target provide a useful diagnostic of axial beam spot size.

METHODS FOR ELECTRON BACKSCATTER

In the radiography application we seek the maximum electron current for a given anode-cathode gap. Therefore current-enhancement effects from ion flow and electron backscatter are of considerable interest. The Trak code was modified to handle electron backscatter from tungsten in the energy range 0.0-1.2 MeV. The Monte Carlo radiation transport code MCNP was used to generate lookup data under the simplifying assumption that the electron emission point was close to its entrance point. We further assumed that the incident electron distribution would be almost symmetrical in azimuth with respect to the local target surface so that variations could be ignored. In this case incident electrons could be described with two parameters: kinetic energy E and $\mu = \cos(\theta)$, where θ is the polar angle with respect to the surface. Similarly, the exit electron is parametrized by E' and μ'. The total backscatter probability P_b was calculated on a 10x10 grid of (E,μ) values. We also calculated marginal probability distributions $P(E',E,\mu)$ and $P(\mu',E,\mu)$ from the coupled probability distribution with similar bins. The data were organized into a standard table format for input to Trak to facilitate future expansion of materials and energy range in the database.

Figure 2 shows how the backscatter data is applied on a conformal mesh. When an incident electron enters a tungsten element, Trak searches for the material/vacuum surface facet intersected by the orbit vector. The incident electron energy E is known while the dot product of orbit and surface normal vectors at the entrance point gives μ. The model particle current is multiplied by P_B. The program determines emission energy and direction by sampling the marginal distributions. The particle is then regenerated with energy E' and direction μ' (relative to the surface normal) at a random value of azimuth.

Electron backscatter may significantly influence current flow in a pinched beam radiation diode. Ion flow is
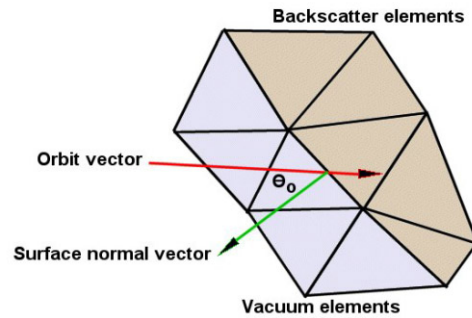

Figure 2. Representing backscatter on a conformal mesh

necessary to support a pinch — the negative space charge of backscattered electrons enhances the flux of ions emitted from the target. Figure 3 shows Trak results for a planar diode (1.0 cm gap, 1.2 MV applied potential) with a tungsten anode. The variation of electric field across the gap is plotted for four cases: 1) bare electrons, 2) electrons and ions, 3) electrons and backscattered electrons and 4) incident and backscattered electrons with ion flow. The presence of ions in the relativistic diode gives an electron-current enhancement factor of 1.96. Without ions the inclusion of the space charge of backscattered electrons gives a suppression factor of 0.85. In contrast, with the feedback mechanism of ion flow the presence of backscattered electrons gives an incident electron current enhancement of 2.89.

NESTED COAXIAL DIODE SIMULATIONS

In the small radiographic diode the goal is to generate high current within the constraints of a practical geometry. The anode-cathode gap must be large enough to avoid plasma closure and to allow latitude for alignment errors. Alignment is a concern because the anode is attached to the cantilevered center-conductor of the magnetically-insulated transmission line. It is also desirable that the diode operates consistently for two or more shots. This feature would allow at least one test shot for a setup. Because the deposited energy density at the anode tip (>10 MJ/kg) is sufficient to vaporize tungsten, the diode design must be tolerant to changes in the anode length.

We studied several cathode configurations for a fixed anode diameter of 1 mm. A hemispherical cathode gave promising results but had several drawbacks. The part required some fabrication effort and the diode performance was sensitive to the relative axial position of the anode tip. Figure 4 shows our present baseline design, the nested coaxial diode. Here the cathode is a thin cylinder of light metal to minimize X-ray attenuation, and there is significant cathode/anode overlap (~5 mm). With the correct choice of cathode radius, electron flow is dominated by magnetic pinching effects creating an anode spot less than 1 mm in length independent of the overlap.
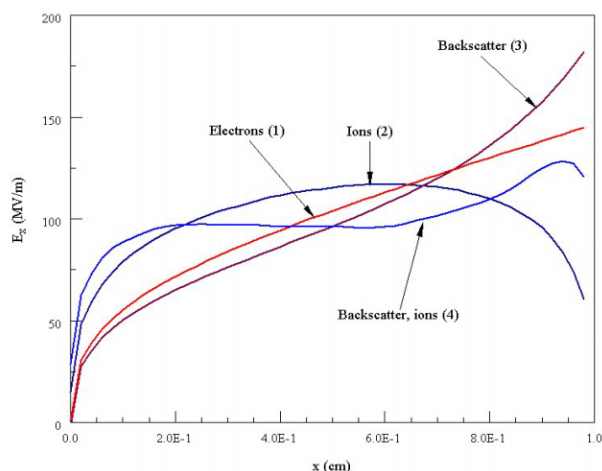
Figure 3. Variation of electric field in a planar diode with incident electrons, ions and backscattered electrons.

In Trak simulations of diode performance a space-charge-limited electron flux was initiated over an extended section of the cathode interior and edge. Ions were emitted from a 2.0 mm length of the anode near the tip. Regarding the origin of the ions, plasma generation is inevitable at the energy densities involved. On the other hand, the plasma initiation time and the ion transit time (3 ns for W^+) may delay the onset of a pinch. It may be necessary to coat the anode with light-ion contaminants. Note that the steady-state simulation results are independent of ion mass.

Table 1 shows scaling of diode behaviour with cathode/anode overlap for a cathode inner-diameter of 10.0 mm and 1.2 MV applied voltage. Electron orbits and variations of the beam-generated magnetic field are shown in Fig. 4. We can draw several conclusions:

1) Even though the overlap and the effective area of the diode varies by a large factor, the total current remains almost constant. The implication is that electron flow in the diode is dominated by magnetic pinch effects.

2) The current initially rises with increasing overlap and then falls. The decrease reflects the fact that ion emission is limited to a small region near the anode tip. At high overlap the ion spray does cover the region of enhanced electric field at the cathode edge.

3) Axial localization of electron deposition improves with both increasing overlap and increasing total current.

4) At 1.2 MV, the critical pinching current in the coaxial diode is about 17 kA.

Table 2 shows results from a set of runs with large anode/cathode overlap (-6.0 mm) as a function of cathode inner diameter. The results have the following implications:

1) The total current does not follow the simple diode scaling with current approximately proportional to the inverse of the square of the gap width. This law predicts that current should increase by a factor 2.25 as the cathode diameter changes from 12.0 mm to 8.0 mm. The simulations show an increase by a factor of only 1.2.

2) Although the change in current with decreasing radius is small, the difference in magnetic pinching force is sufficient to change the electron focal properties substantially. The electron deposition length on the anode drops by a factor of 3.3 at the smaller radius.

In conclusion, the simulations indicate that the nested coaxial diode with a cathode radius <10.0 mm can generate high currents if anode ion generation occurs quickly. The current levels observed (18 kA) are approximately matched to the pulsed-power generator and magnetically-insulated transmission line. At high current electron motion is dominated by magnetic pinching and the axial spot size is less than 1 mm in length.

Table 1. Diode variation with axial overlap

A/K overlap (mm)	I (ka)	Axial size (mm)
0.0	16.58	2.73
1.0	16.16	1.83
2.0	17.19	1.13
3.0	17.29	0.73
4.0	16.67	0.63
5.0	16.52	1.83

Table 2. Diode variation with cathode radius

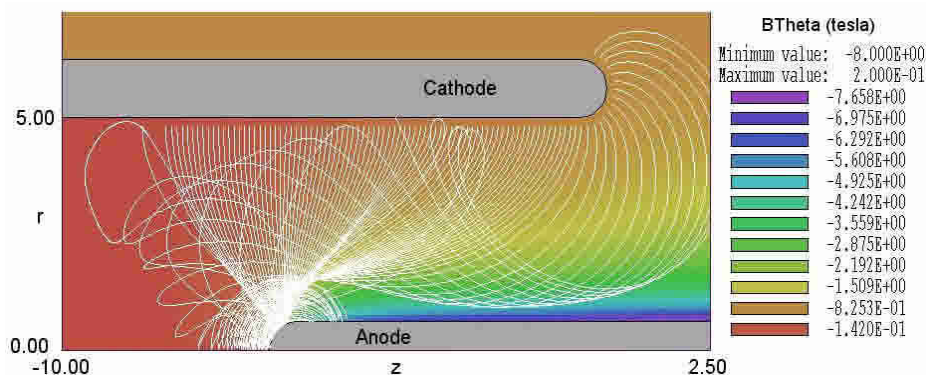| Cathode radius (mm)	I (kA)	Axial size (mm)
6.0	15.19	2.44
5.0	16.14	1.63
4.0	18.17	0.73

Figure 4. Electron orbits and beam-generated magnetic field in the nested coaxial diode.